Aeolian Research 20 (2016) 100–107

Contents lists available at ScienceDirect

Aeolian Research

journal homepage: www.elsevier.com/locate/aeolia

Sandy desertification cycles in the southwestern Mu Us Desert in China over the past 80 years recorded based on nebkha sediments

Jinchang Li [a,*], Yanfang Zhao [a], Haixia Liu [a], Zhizhu Su [b]

[a] Institute of Loess Plateau, Shanxi University, Taiyuan 030006, China
[b] Historical Culture School, Shanxi University, Taiyuan 030006, China

ARTICLE INFO

Article history:
Received 13 August 2015
Revised 23 December 2015
Accepted 24 December 2015
Available online 8 January 2016

Keywords:
Sandy desertification
Nebkha
Westerly circulation
Drought events
Mu Us Desert

ABSTRACT

Sandy desertification (SDN) cycles in the southwestern Mu Us Desert since the late 1920s were recorded based on the evolution of *Nitraria tangutorum* nebkhas. Particle size changes of the nebkha excavated during the study, together with AMS ^{14}C and ^{137}Cs dating controls, indicated that the SDN of the study area was reverse on the whole over the past 80 years, but multiple SDN cycles also occurred. SDN mainly occurred during the late 1920s to the early 1940s, late 1940s to early 1950s, late 1950s to early 1960s, mid- and late 1980s, and early 2000s. The formation of nebkhas in the study area was triggered by severe SDN caused by extreme drought events that occurred in the 1920s to the 1930s. Over the past 80 years, the general SDN trend in the southwestern Mu Us Desert was mainly controlled by the westerly circulation strength, and severe SDN resulted mainly from extreme drought events in a large spatial scale, whereas slight SDN cycles were mainly due to local climate fluctuations and human activities.

1. Introduction

The Mu Us Desert on the southern Ordos Plateau lies at the northern margin of the modern Asian summer monsoon, covering an area of 38,940 km^2, and is an important component of the farming and pastoral zones in Northern China (Fig. 1a). In the UNEP map (1992), the desert is identified as a region of intense sandy desertification (SDN). The main form of SDN in the desert is the evolution of anchored dunes into semi-anchored and mobile dunes, and the main form of reversal is the evolution of mobile dunes into semi-anchored and anchored dunes (Wang et al., 2008a). Given the fragile natural environment and hydrothermal sensitivity of the desert, the historical and modern SDN cycles in the region have received considerable attention over the past several decades (e.g. Huang et al., 2009; Wang et al., 2005).

The SDN cycles in arid and semi-arid regions are mainly presented as the degradation and recovery of vegetation (Thomas and Elias, 2014; Li and Yang, 2014), and is closely associated with regional aeolian activities (Zhang et al., 2012; Yan et al., 2011). Previous studies have also suggested that aeolian activities are important in the development of the aeolian morphology and regional ecological environment (Yizhaq et al., 2013; Wang et al., 2014). Therefore, the variation in the aeolian activities strength can reflect the SDN trend, and the historical SDN cycles can be reconstructed based on the aeolian activity sequences recorded with the aeolian sediments in the arid and semi-arid regions of China (Wang et al., 2008b; Lang et al., 2013a). However, because of the difficulty in acquiring high-resolution aeolian sediments, and the lack of aerial photos and Landsat images before the 1970s, the SDN cycles during the early stage of the previous century remains poorly understood in China.

Our field investigation has found that nebkhas (also referred to as coppice dunes, nabkhas, or vegetated dunes) have developed in the southwestern Mu Us Desert. Nebkhas are produced from aeolian activities (Li et al., 2014), and *Nitraria tangutorum* is found in the nucleus of nearly all the nebkhas in the region. As an incipient nebkha form, *N. tangutorum* traps aeolian sediments, which enlarges the nebkha, and regional environmental changes can be recorded through these sediments (Seifert et al., 2009; Wang et al., 2010; Lang et al., 2013b), thus, the regional SDN cycles can be reconstructed by analysing the sediments deposited within nebkhas. This study uses the particle size of the sediments sampled from a nebkha in the southwestern Mu Us Desert to reconstruct the SDN cycles (with a resolution of one year) of the region over the past 80 years and discuss the association of these cycles with climate change.

* Corresponding author at: No. 92 Wucheng Road, Xiaodian District, Taiyuan, China. Tel.: +86 351 7010700.
E-mail address: lijch@lzb.ac.cn (J. Li).

http://dx.doi.org/10.1016/j.aeolia.2015.12.003
1875-9637/

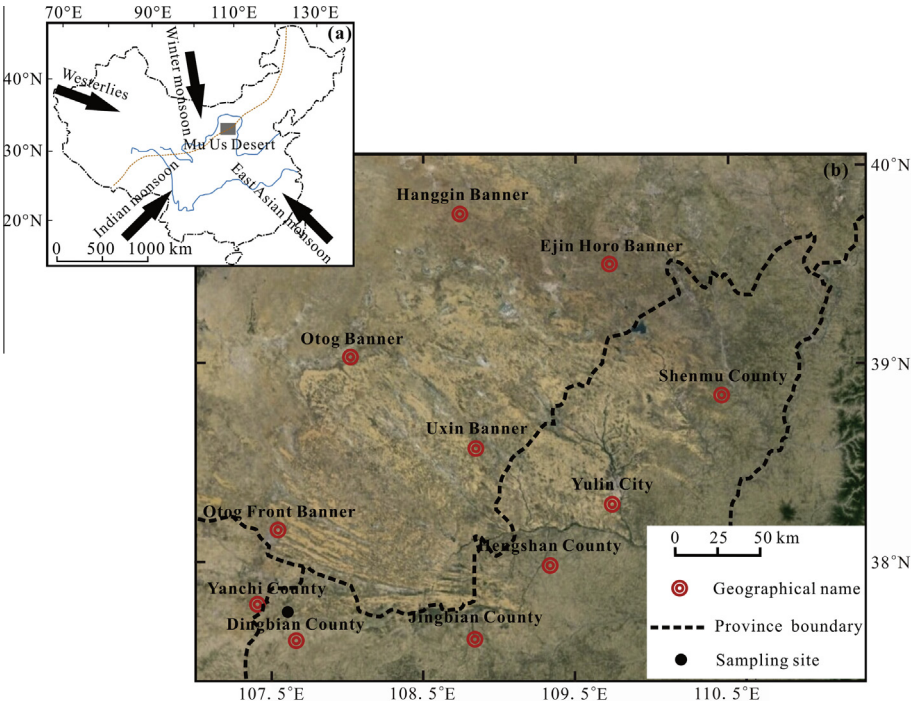

Fig. 1. Location of the study area and sampling site. (a) Mu Us Desert (grey rectangle); the dashed line shows the present limit of the Asian summer monsoon influence, while the blue lines represent the Yellow River and Changjiang River. (b) Google earth screenshot of Mu Us Desert and the sampling site. (For interpretation of the references to colour in this figure legend, the reader is referred to the web version of this article.)

2. Data and methods

2.1. Sampling site

Mu Us Desert has a typical arid and semi-arid continental monsoonal climate with an annual precipitation of 200–400 mm, evaporation of 1800–2500 mm, and aridity of 1.0–2.5 (Liu et al., 2014). This desert currently has a low to moderate wind-energy environment with a ground surface that is dominated by semi-anchored, anchored, and mobile dunes (Wang et al., 2004b). Nebkhas are one of the main types of semi-anchored and anchored dunes in the southwestern Mu Us Desert.

Our sampling site belongs to Dingbian County of Shaanxi Province based on the administrative division (Fig. 1b). According to the instrumental records in the county that has begun in 1976, the mean annual temperature, precipitation and wind velocity are 8.7 °C, 301.5 mm, and 2.5 m s^{-1}, respectively (averaged over the period of 1976–2013), as shown by the trends in Fig. S1 (Supplementary information). In this sampling site, *N. tangutorum* nebkhas extensively develop on the dry riverbeds and previously arable lands, and are almost circular-shaped, aggregative, and clustered (Fig. 2a). The vegetation cover of the nebkhas is approximately 80% to 90% during the growing season (April–October) and 50–60% during the other seasons. The occurrence of wind erosion on the surfaces of the nebkhas is unclear, but previous studies have suggested that when the vegetation cover of the dunes exceeds 14%, the amount of aeolian deposits is greater than the extent of erosion (Wiggs et al., 1994, 1995). In addition, Deng et al. (2007) have suggested that highly obvious environmental changes have not occurred in the desert in recent centuries. Therefore, despite the variations in the vegetation cover during different periods, the regional environment has ensured the continuous development of the nebkhas since the initial formation of these sandy dunes.

On June 14, 2013, we have sampled a *N. tangutorum* nebkha located on a dry riverbed (latitude 37.75°N, longitude 107.61°E, altitude 1306 m). Considering that aeolian sand deposits occur mainly in spring (March–May) in Northern China, the surface sediments of the nebkhas in the region are products of the current year (2013). The nebkha sampled is 240 cm high, 12.2 m in diameter, and round-shaped. The vegetation cover is approximately 80% even at the end of the growing season in late October, and the cover on the southeastern side of the nebkhas is greater than on the other sides because the prevailing winds blow from the northwest. We have excavated the dune to reveal a clean vertical profile through the full depth of the northwestern side. From the crest of the dune toward the bottom, the sediments noticeably consist of aeolian sands entirely (Fig. 2b). We have collected the aeolian sands at 5 cm intervals throughout the profile, and a total of 48 samples has been collected.

2.2. Analytical methods

The *N. tangutorum* litter in the samples at the profile depths of 40, 90, 140, 190, and 240 cm were separated through sieving via accelerator mass spectrometry (AMS) ^{14}C dating. Particle size analysis was performed using a Mastersizer Laser 2000 (Malvern Co. Ltd, Malvern, UK; sample range 0.02–2000 μm in diameter) at the Key Laboratory of Western China Environmental System (Ministry of Education). Before obtaining the particle size measurements, each sample was weighed at 3 g, and the sediments were immersed in 10% H_2O_2, and then in 12.7% HCl to remove any plant debris and disperse the aggregates within the sediments. The sample residue was finally treated with 10 ml of 0.05 M $(NaPO_3)_6$ in an ultrasonic vibrator for 10 min to facilitate the dispersion prior to the particle size analysis. Only slight differences (0.5%) are found in the repeated particles size measurements on each sample.

The AMS ^{14}C dating was performed at the Xi'an AMS Center, Chinese Academy of Sciences. The dating methodology, instrumentation, and calculation of measurement errors as described by Zhou et al. (2007) were followed. The ^{14}C age of each sample was calculated using the methods of Stuiver and Polach (1977), and the ages

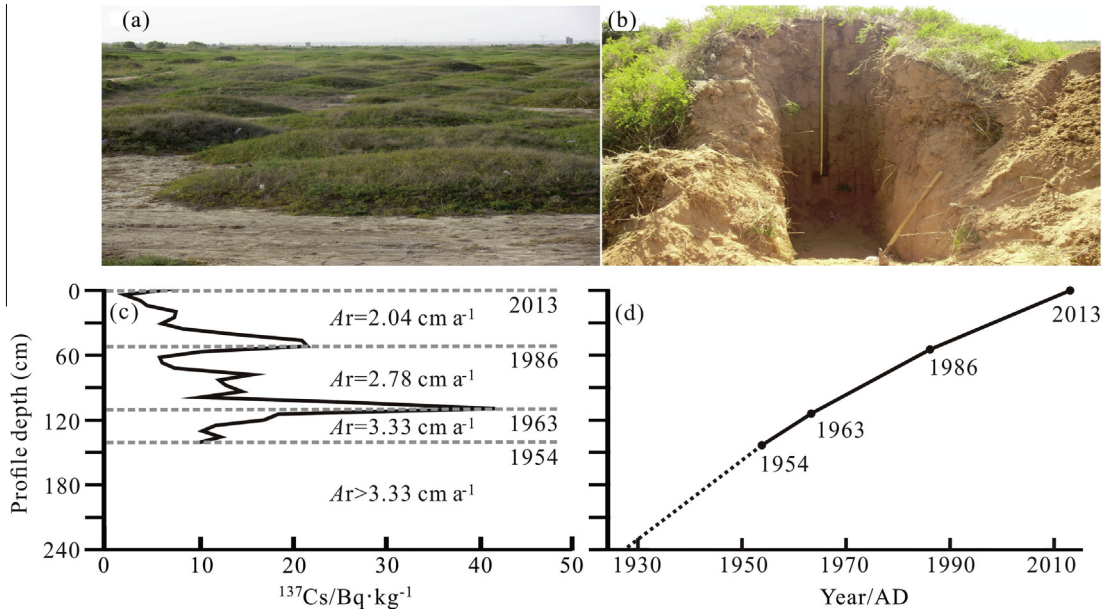

Fig. 2. ^{137}Cs dating results of nebkha in the southwestern Mu Us Desert. (a) Nebkhas in the southwestern Mu Us Desert, (b) profile of the nebkha sampled, (c) location of the ^{137}Cs peak values in the nebkha profile sampled, and (d) the relationship between the profile depth and the years.

were calibrated using Calib 6.1.0 and an IntCal09 calibration data set (Stuiver and Reimer, 1993; Reimer et al., 2009). Before obtaining the ^{137}Cs dating, each sample was air-dried, and then ground enough to pass through a 0.147 mm mesh sieve. From each pretreated sample, a portion of about 10 g was weighted out and placed in a plastic container to measure the ^{137}Cs concentration. The shape of the container was the same as the container of the ^{137}Cs standard reference material supplied by the Institute of Atomic Energy and Sciences, Chinese Academy of Sciences. The ^{137}Cs analysis was conducted at the Institute of Soil Sciences, Chinese Academy of Sciences, using a hyperpure germanium crystal detector (GEM35P, Perkin Elmer Instruments, USA) coupled with a multi-channel gamma-ray spectrometer (DSPEC–CH). The test for each sample lasted for 86,400 s, which provided a measurement precision of between ±5% and 15% at a confidence level of 90%. The ^{137}Cs activities of the samples were calculated by measuring the activity at 662 keV and using the MAESTRO-32 gamma-ray spectrum analysis software (Perkin Elmer Instruments, USA). The ^{137}Cs activity was described based on a mass (Bq kg^{-1}).

The ^{137}Cs dating method was based on the ^{137}Cs accumulation in the sediments, which originated from nuclear tests and nuclear plant accidents that emitted ^{137}Cs into the atmosphere. ^{137}Cs can further precipitate in the sediments, and the peak value of the ^{137}Cs content do not change much regardless of molecular diffusion (Shen et al., 2005). Therefore, the mean accumulation rate can be calculated using the positions of the ^{137}Cs peaks in the profile. The principle of ^{137}Cs dating was described in detail by Zhang et al. (2009). The calculation equation for this methods is as follows:

$$S = (H - h)/(T_1 - T_0), \quad (1)$$

where S (cm a^{-1}) is the mean accumulation rate, H (cm) is the profile depth, h (cm) is the depth of the ^{137}Cs peaks in the nebkha profile, T_1 (a) is the sampling data, and T_0 (a) is the known time when the emission of ^{137}Cs culminated worldwide. The years of the ^{137}Cs culmination were recognised, and that time can correspond to the peak values of the ^{137}Cs content in the profile for dating. The AMS ^{14}C and ^{137}Cs dating methods were successfully used to determine the stratum ages of the nebkhas in the arid Northwestern China (Wang et al., 2010, 2014; Liu et al., 2013).

3. Results

3.1. Chronology

The AMS ^{14}C dating at the different depths of the profile revealed that the buried *N. tangutorum* litters were all modern carbon. ^{137}Cs began to accumulate at the profile depth of 155 cm (Fig. 2c), which dated back to AD 1954, that is the data of the significant deposition level of ^{137}Cs from a nuclear test was first detected in the soil (Robbins et al., 1978). Two other peak values (at the depths of 115 and 55 cm) in the profile dated back to AD 1963 when the world nuclear tests flourished, and AD 1986 during the leakage of Chernobyl Nuclear Power Plant (Fig. 2c) (Appleby et al., 1991). Based on the ^{137}Cs dating results, the mean accumulation rate for the periods of AD 1954 to AD 1963 (at the depth of 155–115 cm) was 3.33 cm a^{-1}. Considering the development was usually fastest during the initial stages of the nebkha (Wang et al., 2010), the mean accumulation rate at the profile depth of 240–155 cm may not be less than 3.33 cm a^{-1}. Therefore, the nebkha originated around late 1920s, that is, the nebkha formed around 80 years ago, which well agreed with the opinion of locals.

Our AMS ^{14}C dating results may be caused mainly by the short growth history of the nebkha. In the Bashang Plateau of China, an AMS ^{14}C dating at the nebkha depth of 130 cm also showed that the buried litter was modern carbon, but the actual age was 80 years (Wang et al., 2006), which resulted from the inherent error of the dating technique. Liu et al. (2014) observed that the Holocene aeolian sediments in the southeastern Mu Us Desert can be divided into 5 aeolian sand layers, 3 palaeosols, 1 weakly developed palaeosol, and 1 sod horizon. However, the nebkha sediments sampled entirely consisted of aeolian sands, which may result from the short formation history of the nebkha, and the generally cold and dry climate of the region for the past 80 years.

The mean accumulation rates for the periods of AD 1963 to 1986 and 1986 to 2013 were 2.78 and 2.04 cm a^{-1}, respectively, and the mean accumulation rate throughout the profile was 2.73 cm a^{-1}, which was slightly less than the mean accumulation rate (3.33 cm a^{-1}) of the nebkha in Alashan Plateau over the past century (Wang et al., 2008b). The average resolution of each sample was 1.79 years with a maximum value of 1.42 years. Therefore,

the chronology of the nebkha profile can be established through linear interpolation between two adjacent ages (Fig. 2d).

3.2. Variation in particle sizes of the nebkha sediments

At different depths of the nebkha profile, the particle size frequency distribution curves all presented an obviously single peak (Fig. 3), the peak values at the different depths varied slightly, and the average value was about 110 μm, which indicated the single source of the nebkha sediments and the aeolian activities strength in the region changed over the past 80 years.

Once the aeolian movement threshold was exceeded and the particles were entrained by the wind, these particles travelled in 5 distinct ways in the order of increasing velocity, namely, creep, saltation, modified saltation, short-term suspension, and long-term suspension, respectively (Pye, 1987). Modified saltation is a means for the particles to travel that lies between pure saltation and pure suspension, and the particles transported this way moved with random trajectory (Pye, 1987). During moderate windstorms, the particles size ranges, particularly those transported through creep, saltation, modified saltation, short-term suspension, and long-term suspension, were >500, 100–500, 63–100, 20–63 and <20 μm, respectively (Pye, 1987). Based on this finding, the particle size ranges of the nebkha sediments were divided.

The content changes in each particle size fraction of the nebkha sediments are shown in Fig. 4. The nebkha sediments did not contain >500 μm fraction throughout the profile, and the average contents of the <20, 20–63, 63–100, and >100 μm fractions were 3.53% (Standard Deviation (SD): 1.95%), 12.38% (SD: 5.12%), 37.66% (SD: 2.55%) and 46.43% (SD: 7.00%), respectively. The coarse sediment contents (>100 μm) evidently decreased, whereas the contents of the <20, 20–63, and 63–100 μm fractions increased as the nebkha developed, but fluctuations were highly apparent. Throughout the profile, the average particle size (APS) varied between 80 and 122 μm, with a mean of 109 μm and an SD of 8 μm. The APS variation in the nebkha sediments was significantly positively correlated with the variation in the coarse fraction (>100 μm). However, this variation was significantly negatively correlated with the variations in the <20, 20–63, and 63–100 μm fractions (Fig. 4, Table 1). These results indicated that saltation was the main means for the particles to travel, and the interdunes and adjacent windward region were the dominant sources of nebkha sediments, as suggested in previous studies (Lancaster, 1995; Wang et al., 2014).

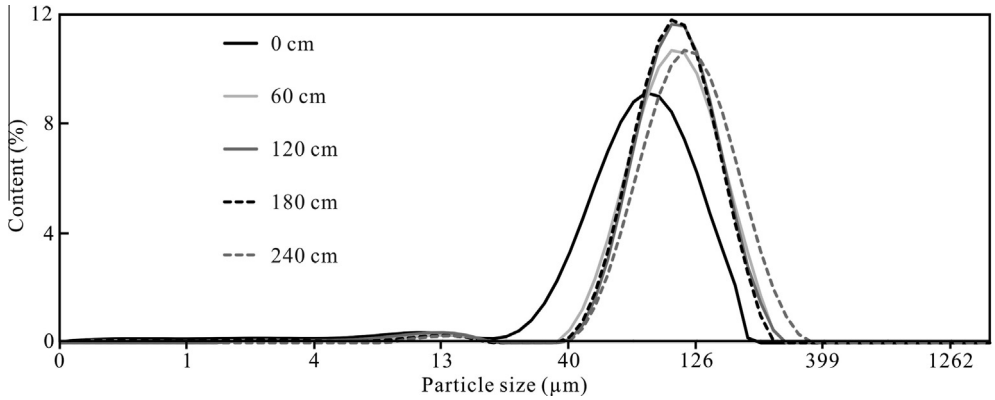

Fig. 3. Particles size frequency distribution at different depths of the nebkha profile sampled.

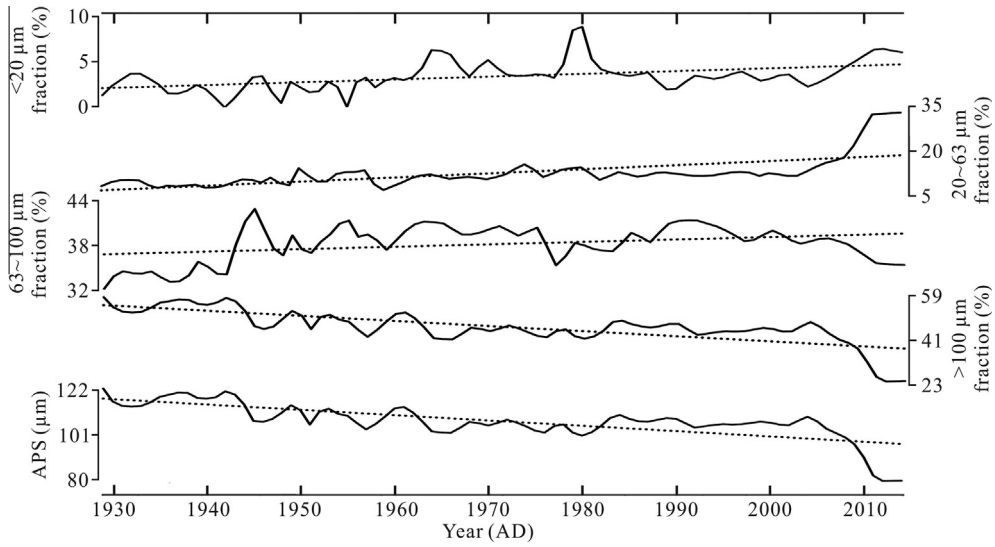

Fig. 4. Variation in each particle size fraction and average particles size (APS) of the nebkha sediments. The annual values were calculated by performing linear interpolation among the measurements.

Table 1
Pearson correlations among the different particles size fractions of the sediments according to the nebkha profile.

	<20 μm	20–63 μm	63–100 μm	>100 μm
20–63 μm	0.495**			
63–100 μm	0.161	0.058		
>100 μm	−0.696**	−0.884**	−0.452**	
APS (μm)	−0.696**	−0.904**	−0.407**	0.998**

* and **indicate the correlation are significant at the 0.05 and 0.01 level, respectively (two-tailed).

3.3. Relationships between the particle size of the nebkha sediments and the modern SDN cycles

Based on a time series of merged NOAA-AVHRR and MODIS images, Karnieli et al. (2014) computed the NDVI of Mu Us Desert from 1981 to 2010. Using TM and MODIS images, Yan et al. (2015) estimated the aboveground biomass (AGB) in the desert from 2000 to 2012. The results of the studies showed that the NDVI and AGB increased generally (Fig. 5), indicating that the SDN of the desert was reverse on the whole during the study period. The coarse fraction and APS of the nebkha sediments exhibited significant anti-correlations with variations in the NDVI (1981–2010) (Pearson correlation coefficients: −0.640 and −0.637; both at the 0.01 level) and AGB (2000–2012) (Pearson correlation coefficients: −0.620 and −0.638; both at the 0.05 level) (Fig. 5).

According to the aerial photos (1:50,000) obtained from the mid-1970s and mid-1980s, Landsat TM images obtained in 2000, and field surveys, Wang et al. (2004a) monitored and reported that the rapid SDN in Mu Us Desert mainly occurred before the mid-1980s and the reversal was significant from the late 1980s to 2000. These reports were also consistent with the coarse fraction and APS variations of the nebkha sediments during these periods (Fig. 4). Therefore, the historical SDN cycles in the southwestern Mu Us Desert since the late 1920s can be reconstructed based on the relationship between the coarse fraction and APS of the nebkha sediments, and the modern SDN trend.

3.4. SDN cycles over the past 80 years in the southwestern Mu Us Desert

Based on the variations in the accumulation rate, coarse fraction, and APS of the nebkha sediments (Figs. 3c and 5), the aeolian activities strength decreased and the SDN reversed on the whole in the southwestern Mu Us Desert since the late 1920s, as identified based on the sediments of Hongjiannao Lake in the northeastern Mu Us Desert (Shen et al., 2005). However, the particle sizes of the nebkha sediments also had obvious fluctuations, which indicated that the southwestern Mu Us Desert experienced multiple SDN cycles, as shown in Fig. 6. SDN occurred mainly during the late 1920s to the early 1940s, late 1940s to early 1950s, late 1950s to early 1960s, mid- and late 1980s, and early 2000s. The worst SDN occurred during the late 1920s to the early 1940s (Fig. 6), indicating that the severe SDN may trigger the formation of nebkhas in the study area. The most notable reversal occurred since mid-2000s (Fig. 6).

4. Discussion

As a nebkha increases in size, the slope angles and height of the nebkha also increase, which raises the threshold of particle entrainment and the grains travelling via saltation become finer (Iversen and Rasmussen, 1994). Suppose that the aeolian activities are stable, the accumulation rate and content of the coarse fraction both decrease without fluctuating as the nebkhas develop. However, previous studies suggested that the accumulation rate and particle size have similar trends with the $\delta^{13}C$ value in the litter and $CaCO_3$ contents of the nebkha sediments (Wang et al., 2008b, 2010; Lang et al., 2013b), and their variations mainly result from the variations in the external environment rather than from the dune height (Wang et al., 2014; Seifert et al., 2009; Lang et al., 2013a). Therefore, the reconstructed SDN cycles of the southwestern Mu Us Desert over the past 80 years have been credible.

Over the past century, as inferred from the lake sediments, ice core sediments, and instrumental annual dust storm frequency, the aeolian activities in Northern China exhibit a weakening trend (Fig. S2, Supplementary information) (Shen et al., 2005; Wang et al., 2007a). Based on tree-ring width chronologies, Hua et al. (2014) have suggested that over the past three centuries, the SDN cycles of the Mongolian Plateau, Northeastern China, and the Yellow River Drainage of China (YRD) have differed because the lagged effects of the responses between the landscape evolution and climate changes vary in each area, and the SDN reversal in the YRD, including Mu Us Desert, has begun after the 1860s and has continued into the present. The field investigations of Wang et al. (2008a) indicate that over the past three decades,

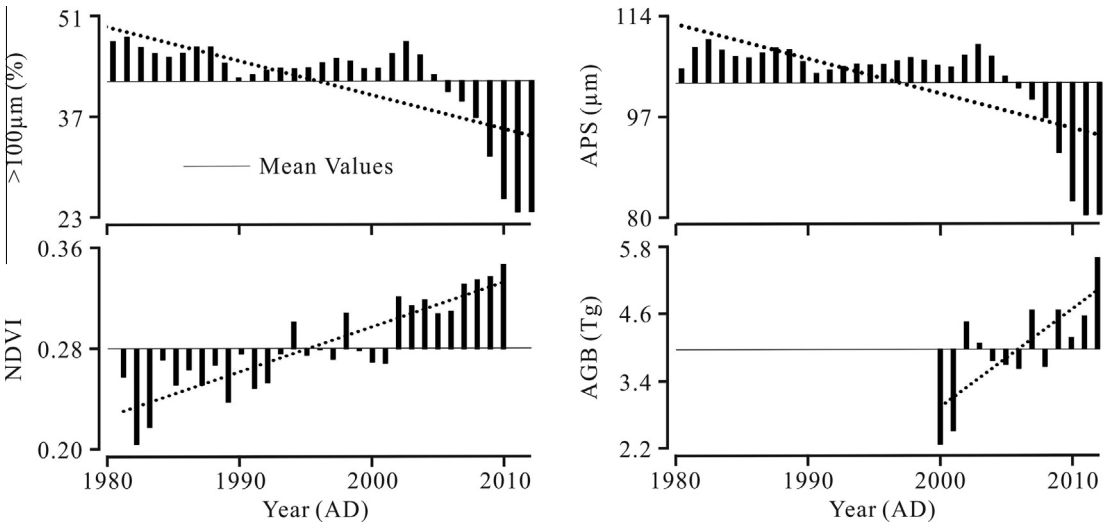

Fig. 5. Variations in the coarse fraction and APS of the nebkha sediments (1981–2010), NDVI (1981–2010), and aboveground biomass (AGB) (2000–2012) in Mu Us Desert. The annual coarse fraction and APS values were calculated by performing linear interpolation among the measurements. The NDVI and AGB data were collected from Karnieli et al. (2014) and Yan et al. (2015), respectively.

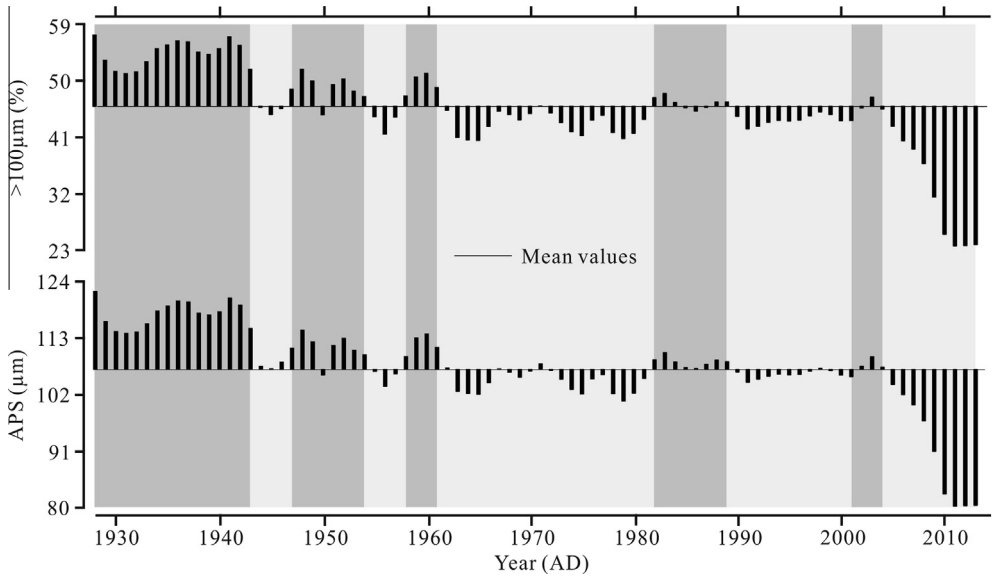

Fig. 6. Variation in the >100 μm fraction and average particles size (APS) of the sediments based on the nebkha profile. The key phases of sandy desertification and reversals derived from the aeolian activities strength are indicated by the dark grey and light grey shadings, respectively. The annual values were calculated by performing linear interpolation among the measurements.

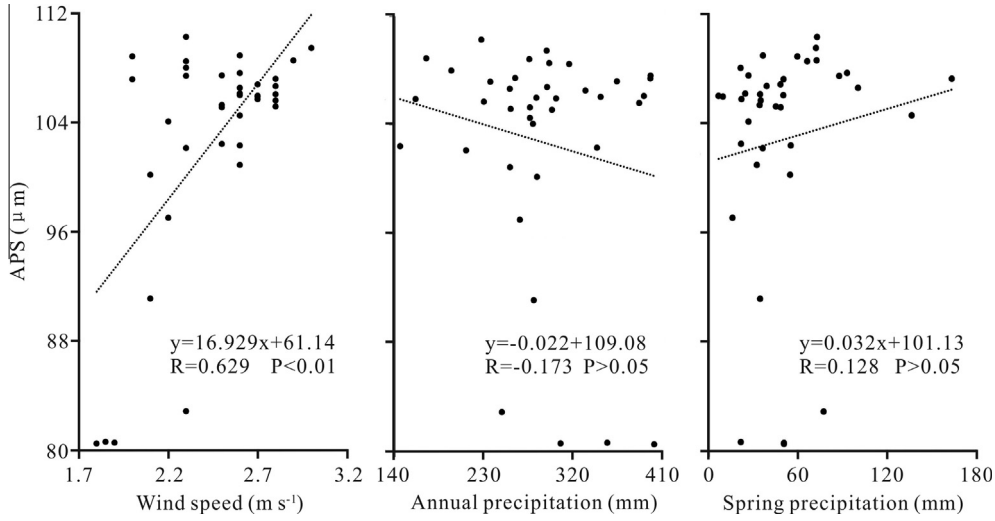

Fig. 7. Scatter between the APS of the nebkha sediments and the meteorological factor trends as recorded by the Dingbian meteorological station from 1976 to 2013. The location of Dingbian County identified in Fig. 1b. The annual APS was calculated by performing linear interpolation among the measurements.

mobile dunes have been replaced by semi-anchored or anchored dunes, and semi-anchored dunes have been replaced by anchored dunes considerably in most deserts in Northern China. These findings indicate that SDN has been reversed on the whole over the past 80 years, not only in the southwestern Mu Us Desert but also in the other arid and semi-arid regions in China, which may result mainly from the decreased wind speed because of the weakening westerly circulation strength and winter monsoon caused by global warming (Wang et al., 2007b; He, 2013). Fig. 7 also shows that from 1976 to 2013, the APS of the nebkha sediments has a similar trend with the annual wind speed, given the Pearson correlation coefficients of 0.629 (at the 0.01 level) in the southwestern Mu Us Desert. Previous studies have also suggested that the decrease in wind speed can benefit soil and water conservation, vegetation growth, and soil formation by decreasing the vulnerability of land to erosion (Zobeck and Fryrear, 1986).

Although the reversal of the SDN in the YRD continued from the 1860s to the present, the severe SDN occurred during the 1920s and the 1930s (Hua et al., 2014), which were the periods when nebkhas began to form and the worst SDN has occurred in the southwestern Mu Us Desert over the past 80 years. During the 1920s and 1930s, the aeolian activities in Northern China have notably increased (Fig. S2, Supplementary information) and a severe SDN is also observed in the southeastern Mongolia Plateau (Lang et al., 2013a). Although no obvious increase or decrease trends are observed in the total annual precipitation in the arid and semi-arid regions of China over the past few decades (Ding et al., 2006), based on a network of tree-ring data and historical documents, Liang et al. (2006) have suggested that a severe and sustained drought has occurred in the regions during the 1920s and 1930s. These suggestions indicate that the occurrence of a severe SDN is synchronous in the arid and semi-arid regions of China,

and may be caused mainly by the extreme drought events with large spatial scale, causing vegetation loss, aeolian deflation, and dune deposition. The nebkhas in the forested region of South Central United States (Seifert et al., 2009) and in the Alashan Plateau of China (Wang et al., 2010) are also regarded to have formed during historical extreme drought periods. Fig. 7 shows that although the correlation between the APS of the nebkha sediments and the annual precipitation from 1976 to 2013 is insignificant, but the remarkably low annual precipitations are synchronous with the large APS, which further suggests that a dry climate can trigger the enhancement of aeolian activities and the occurrence of severe SDN. Wang et al. (2007b) have proposed that spring precipitation may have a significant impact on SDN, but lacked detailed analysis. Fig. 7 shows that annual precipitation may have a greater effect on the SD than spring precipitation in the study area.

Based on the analysis on the geochemical elements of the nebkha sediments in the southeastern Mongolia Plateau, Lang et al. (2013a) have reported that over the past 80 years, SDN in the region has mainly occurred during the late 1930s to early 1950s, late 1950s to late 1960s, mid-1970s, mid-1980s to early 1990s, and late 1990s to mid-2000s, which are slightly different compared with our findings in the southwestern Mu Us Desert (Fig. 6). Over the past three decades, the inter-annual NDVI in Mu Us Desert and in the other arid and semi-arid regions of China exhibit similar increasing trends, except for a few phases (Karnieli et al., 2014; Wu et al., 2014; An et al., 2014). These findings may indicate that the slight fluctuation in the SDN of the southwestern Mu Us Desert is regional, and is controlled mainly by local climate fluctuations and human activities.

Although previous studies have proposed that the SDN cycles in Mu Us Desert result from significant human impacts (Wu, 2001; Wu and Ci, 2002), insufficient evidence is provided in these studies to support this hypothesis, and the several desertification and reversal phases that have occurred in this region over the past three decades remain unexplained. Based on the results of systematic monitoring, and the contemporaneous climate and human impacts, Wang et al. (2005) have suggested that the SDN cycles in Mu Us Desert are primarily triggered by climate changes, even though human impacts have undeniably exacerbated their effects. Our study has also revealed that over the past 80 years, the general SDN trend in the southwestern Mu Us Desert is controlled mainly by the westerly circulation strength, and the severe SDN results mainly from the extreme drought events with large spatial scales, whereas the slight SDN cycles are caused mainly by local climate fluctuations and human activities.

5. Conclusions

In this study we determined the changes of particle size in one nebkha profile from the southwestern Mu Us Desert, China. We used these data, together with AMS ^{14}C and ^{137}Cs dating controls, to reconstruct the sand desertification cycles since the late 1920s. The results of this study can be summarized as follows:

- The SDN of the study area was reverse on the whole over the past 80 years, but multiple SDN cycles also occurred. SDN mainly occurred during the late 1920s to the early 1940s, late 1940s to early 1950s, late 1950s to early 1960s, mid- and late 1980s, and early 2000s.
- The formation of nebkhas in the study area was triggered by severe SDN caused by extreme drought events that occurred in the 1920s to the 1930s. Over the past 80 years, the general SDN trend in the southwestern Mu Us Desert was mainly controlled by the westerly circulation strength, and severe SDN resulted mainly from extreme drought events in a large spatial scale, whereas slight SDN cycles were mainly due to local climate fluctuations and human activities.

Acknowledgments

This study was supported by the Science & Technology Pillar Program of Shanxi Province (No. 20121101011), the Soft Science Project of Shanxi Province (No. 2015041020-1), and the National Natural Science Foundation of China (Nos. 41330748, 41271030).

Appendix A. Supplementary data

Supplementary data associated with this article can be found, in the online version, at http://dx.doi.org/10.1016/j.aeolia.2015.12.003.

References

An, Y.Z., Gao, W., Gao, Z.Q., 2014. Characterizing land condition variability in Northern China from 1982 to 2011. Environ. Earth Sci. 72, 663–676.
Appleby, P.G., Richardson, N., Nolan, P.J., 1991. ^{241}Am dating of lake sediments. Hydrobiologia 214, 35–42.
Deng, H., Shu, S.G., Song, Y.Q., Xing, F.L., 2007. Distribution of sand dunes and sand shifts along the southern fringe of the Mu Us Desert since the Ming Dynasty. Chin. Sci. Bull. 52 (22), 3128–3138.
Ding, Y., Ren, G., Shi, G., 2006. National assessment report of climate change (1): climate change in China and its future trend. Adv. Clim. Change Res. 2, 3–8 (in Chinese).
He, S.P., 2013. Reduction of the East Asian winter monsoon interannual variability after the mid-1980s and possible cause. Chin. Sci. Bull. 58 (12), 1331–1338.
Hua, T., Wang, X.M., Lang, L.L., Zhang, C.X., 2014. Variations in tree-ring width indices over the past three centuries and their associations with sandy desertification cycles in East Asia. J. Arid Environ. 100–101, 93–99.
Huang, Y.Z., Wang, N.A., He, T.H., Chen, H.Y., Zhao, L.Q., 2009. Historical desertification of the Mu Us Desert, Northern China: A multidisciplinary study. Geomorphology 110 (3–4), 108–117.
Iversen, J.D., Rasmussen, K.R., 1994. The effect of surface slope on saltation threshold. Sedimentology 41, 721–728.
Karnieli, A., Qin, Z.H., Wu, B., Panov, N., Yan, F., 2014. Spatio-temporal dynamics of land-use and land-coverin the Mu Us Sandy Land, China, using the change vector analysis technique. Remote Sens. 6 (10), 9316–9339.
Lancaster, N., 1995. Geomorphology of Desert Dunes. Routledge Press, London.
Lang, L.L., Wang, X.M., Hua, T., Ha, S., 2013a. Nebkha formation and its significance to desertification reconstructions in the southeastern Mongolia Plateau. Quat. Sci. 33 (2), 325–333 (in Chinese).
Lang, L.L., Wang, X.M., Hua, T., Zhang, C.X., 2013b. Moisture availability over the past five centuries indicated by carbon isotopes of Tamarix taklamakanensis leaves in a nebkha profile in the Central Taklimakan Desert, NW China. Aeolian Res. 11, 101–108.
Li, H.W., Yang, X.P., 2014. Temperate dryland vegetation changes under a warming climate and strong human intervention-with a particular reference to the district Xilin Gol, Inner Mongolia, China. Catena 119, 9–20.
Li, J.C., Gao, J., Zou, X.Y., Kang, X.Y., 2014. The relationship between nebkha formation and development and desert environmental changes. Acta Ecolog. Sin. 34 (5), 266–270.
Liang, E., Liu, X., Yuan, Y., Qin, N.S., Fang, X.Q., Huang, L., Zhu, H.F., Wang, L., Shao, X. M., 2006. The 1920s drought recorded by tree rings and historical documents in the semi-arid and arid areas of northern China. Clim. Change 79, 403–432.
Liu, Q., Gao, C.J., Zhao, Y.J., Xia, X.C., 2013. Positive ion contained in tamarix cone sedimentary veins and climatic and environmental change in southern region of the Taklimakan desert. Adv. Earth Sci. 28 (12), 1326–1334.
Liu, B., Jin, H.L., Sun, L.Y., Sun, Z., Niu, Q., Xie, S.B., Li, G.H., 2014. Holocene moisture change revealed by the Rb/Sr ratio of aeolian deposits in the southeastern Mu Us Desert, China. Aeolian Res. 13, 109–119.
Pye, K., 1987. Aeolian Dust and Dust Deposits. Academic Press, London.
Reimer, P.J., Baillie, M.G.L., Bard, E., Bayliss, A., Beck, J.W., Blackwell, P.G., Ramsey, C. B., Buck, C.E., Burr, G.S., Edwards, R.L., Friedrich, M., Grootes, P.M., Guilderson, T. P., Hajdas, I., Heaton, T.J., Hogg, A.G., Hughen, K.A., Kaiser, K.F., Kromer, B., McCormac, F.G., Manning, S.W., Reimer, R.W., Richards, D.A., Southon, J.R., Talamo, S., Turney, C.S.M., van der Plicht, J., Weyhenmeyer, C.E., 2009. IntCal09 and Marine09 radiocarbon age calibration curves, 0–50,000 years cal BP. Radiocarbon 51, 1111–1150.
Robbins, J.A., Edgington, D.N., Kemp, L.W., 1978. Comparative ^{210}Pb, ^{137}Cs, and pollen geochronologies of sediments from Lake Ontario and Erie. Quat. Res. 10, 256–278.
Seifert, C.L., Cox, R.T., Forman, S.L., 2009. Relict nebkhas (pimple mounds) record prolonged late Holocene drought in the forested region of south-central United States. Quat. Res. 71, 329–339.

Shen, J., Wang, Y., Yang, X.D., Zhang, E.L., Yang, B., Ji, J.F., 2005. Paleosandstorm characteristics and lake evolution history deduced from investigation on lacustrine sediments—The case of Hongjiannao Lake, Shaanxi Province. Chin. Sci. Bull. 50 (20), 2355–2361.
Stuiver, M., Polach, H.A., 1977. Discussion: reporting of ^{14}C data. Radiocarbon 19, 355–363.
Stuiver, M., Reimer, P.J., 1993. Extended ^{14}C data base and revised CALIB 3.0 ^{14}C age calibration program. Radiocarbon 35, 215–230.
Thomas, H., Elias, S., 2014. Assessing land degradation and desertification using vegetation index data: current frameworks and future directions. Remote Sens. 6 (10), 9552–9575.
UNEP (United Nations Environment Programme), 1992. World Atlas of Desertification. Edward Arnold, London.
Wang, T., Wu, W., Xue, X., Han, Z.W., Zhang, W.M., Sun, Q.W., 2004a. Spatial-temporal changes of sandy desertified land during last 5 decades in northern China. Acta Geogr. Sin. 59, 203–212.
Wang, X.M., Dong, Z.B., Yan, P., Zhang, J.W., Qian, G.Q., 2004b. Wind energy environments and dunefield activity in the Chinese deserts. Geomorphology 65 (1), 33–48.
Wang, X.M., Chen, F.H., Dong, Z.B., 2005. Evolution of the southern Mu Us Desert in north China over the past 50 years: an analysis using proxies of human activity and climate parameters. Land Degrad. Dev. 16, 351–366.
Wang, X.M., Wang, T., Dong, Z.B., Liu, X.P., Qian, G.Q., 2006. Nebkha development and its significance to wind erosion and land degradation in semi-arid northern China. J. Arid Environ. 65 (1), 129–141.
Wang, N.L., Yao, T.D., Yang, X.D., Shen, J., Wang, Y., 2007a. Variations in dust event frequency over the past century reflected by ice-core and lacustrine records in north China. Sci. China (Ser. D) 50 (5), 736–744.
Wang, X.M., Eerdun, H.S., Zhou, Z.J., Liu, X.P., 2007b. Significance of variations in the wind energy environment over the past 50 years with respect to dune activity and desertification in arid and semiarid northern China. Geomorphology 86 (3–4), 252–266.
Wang, X.M., Chen, F.H., Hasi, E.D., Li, J.C., 2008a. Desertification in China: an assessment. Earth-Sci. Rev. 88, 188–206.
Wang, X.M., Xiao, H.L., Li, J.C., Qiang, M.R., Su, Z.Z., 2008b. Nebkha development and its relationship to environmental change in the Alaxa Plateau. China Environ. Geol. 56, 359–365.
Wang, X.M., Zhang, C.X., Zhang, J.W., Hua, T., Lang, L.L., Zhang, X.Y., Wang, L., 2010. Nebkha formation: implications for reconstructing environmental changes over the past several centuries in the Ala Shan Plateau. China. Palaeogeogr. Palaeocl. 297 (3–4), 697–706.
Wang, X.M., Lang, L.L., Hua, T., Zhang, C.X., Li, H., 2014. Variations in the wind-energy regiome of the Takelimakan Desert, central Asia, over the last 700 years as inferred from nebkha sedimentology and chronology. Boreas 43 (4), 882–894.
Wiggs, G.F.S., Livingstone, I., Thomas, D.S.G., Bullard, J.E., 1994. Effect of vegetation removal on airflow patterns and dune dynamics in the southwest Kalahari Desert. Land Degrad. Dev. 5, 13–24.
Wiggs, G.F.S., Thomas, D.S.G., Bullard, J.E., Livingstone, L., 1995. Dune mobility and vegetation cover in the southwest Kalahari Desert. Earth Surf. Proc. Land. 20, 515–529.
Wu, W., 2001. Study on processes of desertification in Mu Us Sandy Land for last 50 years, China. J. Desert Res. 21, 164–169 (in Chinese).
Wu, B., Ci, L.J., 2002. Landscape change and desertification development in the Mu Us Sandland, Northern China. J. Arid Environ. 50, 429–444.
Wu, Z.T., Wu, J.J., He, B., Liu, J.H., Wang, Q.F., Zhang, H., Liu, Y., 2014. Drought offset ecological restoration program-induced increase in vegetation activity in the Beijing-Tianjin sand source region, China. Environ. Sci. Technol. 48, 12108–12117.
Yan, Y.C., Xu, X.L., Xin, X.P., 2011. Effect of vegetation coverage on Aeolian dust accumulation in a semiarid steppe of northern China. Catena 87 (3), 351–356.
Yan, F., Wu, B., Wang, Y.J., 2015. Estimating spatiotemporal patterns of aboveground biomass using Landsat TM and MODIS images in the Mu Us Sandy Land, China. Agr. Forest Meteorol. 200, 119–128.
Yizhaq, H., Ashkenazy, Y., Levin, N., Tsoar, H., 2013. Spatiotemporal model for the progression of transgressive dunes. Physica A 392 (19), 4502–4515.
Zhang, Y., Gao, X., Zhong, Z.Y., Chen, J., Peng, B.Z., 2009. Sediment accumulation of Dianchi Lake determined by ^{137}Cs dating. J. Geogr. Sci. 19, 225–238.
Zhang, F.F., Zhang, H.Y., Huang, T.S., 2012. Dynamics on the interaction between vegetation growth an aeolian dust deposition. Adv. Mater. Res. 1479 (356), 2430–2433.
Zhou, W.J., Lu, X.F., Wu, Z.K., Zhao, W.N., Huang, C.H., Li, L.L., Peng, C., 2007. The AMS facility at Xi'an AMS Centre. Nucl. Technol. 30 (8), 702–708.
Zobeck, T.M., Fryrear, D.W., 1986. Chemical and physical characteristics of windblown sediment: chemical characteristics and nutrient discharge. Trans. ASAE 29, 1032–1036.